Desalination and Water Treatment
www.deswater.com
doi: 10.1080/19443994.2014.982199

57 (2016) 3218–3226
February

Taylor & Francis
Taylor & Francis Group

Adsorptive removal of acid orange 7 from aqueous solution with metal–organic framework material, iron (III) trimesate

Fang-Chang Tsai[a,*], Yue Xia[a], Ning Ma[a], Jing-Jing Shi[a], Tao Jiang[a], Tai-Chin Chiang[b], Zuo-Cai Zhang[a], Wen-Chin Tsen[c]

[a]*Ministry-of-Education Key Laboratory for the Green Preparation and Application of Functional Materials, Faculty of Materials Science and Engineering, Hubei University, 368 Youyi Avenue, Wuchang, Wuhan 430062, Hubei, P.R. China, Tel. +86 27 88661729; Fax: +86 88661729; email: tfc0323@gmail.com (F.-C. Tsai)*
[b]*Graduate School of Materials Science and Engineering, National Taiwan University of Science and Technology, No. 43, Sec. 4, Keelung Rd., Da'an Dist., Taipei 10607, Taiwan, ROC*
[c]*Department of Fashion and Design, Lee-Ming Institute of Technology, No. 2-2, Lizhuan Rd., Taishan Dist., New Taipei 24305, Taiwan, ROC*

Received 26 July 2014; Accepted 25 October 2014

ABSTRACT

In this paper, a highly porous metal–organic framework (MOF) based on iron (III) trimesate (MIL-100 (Fe)) was applied to the adsorption of a harmful anionic dye, acid orange 7 (AO7), from aqueous solution. The influences of various factors on the adsorption as well as adsorption kinetics and isotherms were investigated. It was found that a relatively low pH value was favorable for the adsorption. The high dosage of the adsorbent led to a high decolorization rate, but a low adsorption quantity. The adsorption kinetics obeyed the pseudo-second-order kinetic model and the adsorption isotherms followed the Langmuir mode. The driving force of the adsorption was an entropy effect rather than an enthalpy change. The adsorption mechanism may be explained with a simple electrostatic interaction between AO7 aqueous solution and the adsorbent. The adsorption capacities of MIL-100 (Fe) are much higher than those of an activated carbon. Finally, it can be suggested that (MOFs) having high porosity and large pore size can be potential adsorbents to remove harmful AO7 in contaminated water.

Keywords: Metal–organic framework; Dye; Adsorption; Acid orange 7; Wastewater treatment

1. Introduction

Recently, a large amount of wastewater containing organic dyes is produced by industries such as textile, paper, leather, and plastics in which dyes are used to color their products [1,2]. It is difficult to biodegrade dyes in wastewater due to the fact that dyes have a synthetic origin and a complex aromatic molecular structure which make them stable [3]. Traditionally, there are three main categories for the removal of dye materials from contaminated water, that is, biological [4], physical [5,6], and chemical [7,8] method. Among these methods, physical adsorption is generally considered to be the most efficient method for quickly lowering the concentration of dissolved dyes in wastewater [9].

*Corresponding author.

Metal–organic frameworks (MOFs) are a promising class of porous crystalline materials constructed by metal ions (or clusters) connected by various organic ligands, which have a diverse structure and compositions, large porosity and surface area, tunable pore size, biological compatibility, and so on [10–12]. MOFs are showing a great potential for application in separations, catalysis, gas storage, drug delivery [13]. As a unique kind of adsorbent, MOFs used for the removal of hazardous materials such as nitrogen-containing compounds [14], sulfur-containing compounds [15], dyes [16,17], pesticide [18], volatile organic compounds [19], harmful gas [20], and heavy metals [21] have been reported.

In 2004, Chae et al. [22] synthesized a novel type of MOFs (MOF-177) with high surface area and ordered structure, which had extra-large pores capable of binding polycyclic organic guest molecules, and they reported the movement and distribution of organic dyes in MOFs firstly. And then, in 2010, for the first time, the usage of MOFs in the removal of dyes was reported; MIL-101 (Cr) was suggested to have high adsorption capacity for the removal of anionic dye methyl orange (MO), especially when MIL-101 (Cr) was protonated ethylenediamine-grafted due to a specific interaction like electrostatic interaction between MO and adsorbent [16]. MOFs were also investigated for the adsorption of other organic dyes, such as uranine [23], xylenol orange (XO) [24], malachite green (MG) [25], and MB [26]. In general, MOFs showed an excellent adsorption of dyes over a wide concentration range, and the adsorption saturation was much greater than traditional adsorbents like MCM-41 and active carbon [27]. However, there are still few reports about the dye adsorption on MIL-100, so that more work and examples are needed for further study.

As azo dyes are the largest group of colorant, acid orange 7 (AO7) has been used in several industries. The structure of AO7 is shown in Fig. 1. AO7 is carcinogenic and the ingestion of AO7 is proved fatal and will lead to skin, mucous membrane, eye, and upper respiratory tract irritation [28]. There have been many reports on the adsorption of AO7 [28–31], but the adsorption rate or the adsorption quantity is relatively low in these researches (shown in Table S3 in supplementary material). In this work, MOFs were used to remove AO7, the influences of various factors on the adsorption as well as the adsorption kinetics and isotherms were investigated. MIL-100 (Fe) was expected to have a quick and efficient adsorption. It may provide a new method for rapid decolorization of organic dye and may put forward a rational design of advanced MOFs-based adsorbent for environmental recovery.

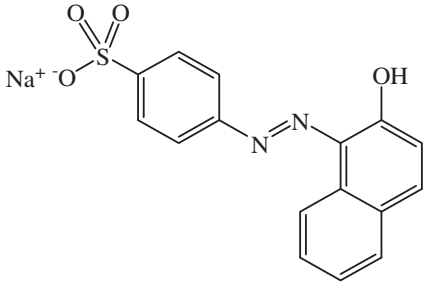

Fig. 1. The structural formula of acid orange 7.

2. Experimental

All general reagents and solvents are commercially available and used without further purification. Iron powder (99.9%, 25 nm, Junye Nano Materials Co., Ltd), 1,3,5-benzenetricarboxylic acid (trimesic acid, $H_3BTC > 99\%$, Shanghai Dibo Chemicals Co., Ltd), nitric acid (AR, 65–68%, Sinopharm Chemical Regent Co., Ltd), hydrofluoric acid (AR > 40%, Sinopharm Chemical Regent Co., Ltd), and ultrapure water (11.5 MΩ cm) obtained from a water purification system were used to prepare MIL-100 (Fe). AO7 ($C_{25}H_{30}N_3Cl$) > 98%) and ethanol (AR > 99.7%) were purchased from Sinopharm Chemical Regent Co., Ltd.

A pH meter pHS-3C (Hangzhou, China) was used to measure the pH values. A conductivity meter DDS-12A (Shanghai, China) was used to determine the conductivity of the mother liquor. A spectrophotometer UV762 (Shanghai, China) was used for determining the concentration of AO7 aqueous solution at the wavelength of 496 nm. JSM6510LV scanning electron microscope (SEM) (Hitachi, Japan) was used to get the SEM images. A ZEN3600 laser particle size analyzer (Malvem, Britain) was used to measure the zeta potential of the adsorbent. Bruker D8 focus diffractometer was used to record the power X-ray diffraction patterns with the 2θ range from 5° to 40° using Cu Kα radiation. V-Sorb 2800 TP surface area and pore size analyzer (Beijing, China) were used to measure the N_2 adsorption–desorption isotherms of samples at 77 K.

MIL-100 (Fe) was synthesized according to the published work by Yoon et al. [32]. Briefly, iron powder (0.515 g), H_3BTC (1.295 g), hydrofluoric acid (35%, 0.4 mL), and nitric acid (65%, 0.7 mL) were mixed well with ultrapure water (50 mL) in a Teflon-lined steel autoclave. The autoclave was then placed in an oven, which was progressively heated to 150℃ from room temperature in 1 h and then maintained at 150℃ for 12 h. Then the oven was cooled down to room

temperature in 24 h. After cooling down, the light orange solid product was collected by filtration and then washed with ultrapure water for three times. The as-synthesized MIL-100 (Fe) was further purified with boiling water at 80°C for 6 h to remove residual unreacted ions, and then with hot ethanol at 60°C for 3 h until the conductivity of the mother liquor decreased to 1.0 mS cm^{-1} (the conductivity of ethanol was 0.84 mS cm^{-1}). The highly purified MIL-100 (Fe) was then collected by centrifugation at 4,000 rpm for 10 min. The solid was finally dried at 80°C under vacuum for 24 h.

An aqueous stock solution of AO7 (1,000 ppm) was prepared by dissolving AO7 in ultrapure water and then stored in the dark. Different concentrations of AO7 aqueous solutions were prepared by step-by-step dilution of the stock solution with ultrapure water before use. Before adsorption, the MIL-100 (Fe) was dried at 80°C overnight under vacuum and was kept in a desiccator. In order to determine the effect of aqueous solution pH on the adsorption capacity of dye on MIL-100 (Fe), the pH of the dye solution was adjusted with 0.1 M HCl or 0.1 M NaOH aqueous solution, the initial concentration of AO7 was 30 ppm, and the contact time was 24 h. Then the dosage of adsorbent for adsorption was carried out to determine a suitable adsorbent concentration.

The aqueous AO7 solution (10 mL) having fixed with dye concentrations from 10 ppm to 500 ppm and an exact amount of the MIL-100 (Fe) (~4 mg) were put into a 25 mL centrifuge plastic tube and then put in the oven at a fixed temperature. After adsorption for a predetermined time, the supernatants were separated from the adsorbent by centrifugation (4,000 rpm, 5 min) and the dye concentration of obtained supernatants was determined by a UV–vis spectra, then the amount of adsorbed dye on adsorbent was calculated by the following Eq. (1):

$$q_e = \frac{(C_0 - C_e)V}{m} \quad (1)$$

where q_e: the amount of dye adsorbed at equilibrium (mg g^{-1}), C_0: the initial dye concentration in liquid phase (mg L^{-1}), C_e: the liquid-phase dye concentration at equilibrium (mg L^{-1}), V: the volume of dye solution (L), and m: the mass of adsorbent (AO7) (g).

3. Results and discussion

3.1. Characterization results

The well-defined diffraction peaks in the XRD figures in Supporting Fig. S1 revealed the high crystallinity of the sample and they matched well with previous literature [25,32,33], illustrating that the framework of the synthesized material has the structure of MIL-100 (Fe). The SEM image of the as-synthesized MIL-100 (Fe) in Supporting Fig. S2 indicated that the MIL-100 (Fe) had homogeneous morphology. It was suggested that MIL-100 (Fe) was successfully synthesized.

The N_2 adsorption–desorption isotherms at 77 K for as-synthesized MIL-100 (Fe) and MIL-100 (Fe) after adsorbing AO7 was shown in Supporting Fig. S3, and the corresponding specific surface area and the pore volume were shown in Supporting Table S1. Both the Brunauer–Emmett–Teller (BET) surface area and Langmuir surface area were deceased after adsorbing AO7. The pore volume decreased from 0.79 $cm^3 g^{-1}$ to 0.49 $cm^3 g^{-1}$, suggesting that the AO7 may entered into the framework of the adsorbent.

3.2. Effect of pH

As the ratio of H^+/OH^- in aqueous solution affects the structure of a dye as well as the charge characteristic of an adsorbent MOFs, the adsorption of a dye usually highly depends on the pH value of the dye solution. To establish the effect of initial solution pH on AO7 adsorption on MIL-100 (Fe), the adsorption experiments were carried out at 30 ppm dye concentration with adsorbent concentration of 0.4 mg mL^{-1} at 298 K for 24 h equilibrium time in this work. As shown in Fig. 2, the AO7 decolorization dropped down from 96.22% to 77.11% as the pH value increased from 3 to 10. The decolorization ratio decreased with the increasing of the initial pH value of AO7 solution, which might be due to the fact that the concentration of negative charge of adsorbents

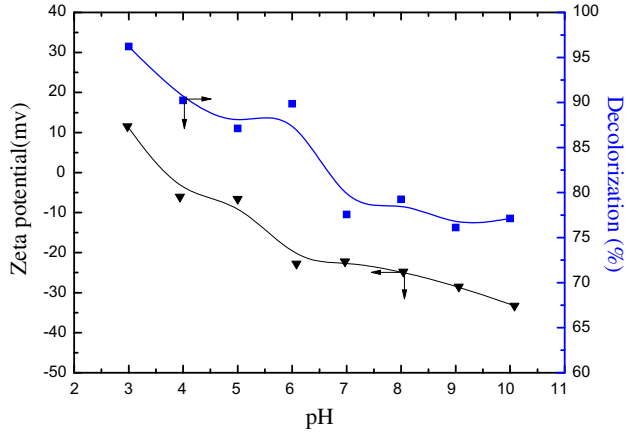

Fig. 2. Effect of the pH value on the zeta potential of MIL-100 (Fe) and the decolorization of AO7.

increased with increasing pH, as which were shown in the zeta potential dates. As described above, AO7 in an anionic dye, the negative charge on the surface of MIL-100 (Fe) impeded the movement of AO7 into the interior of metal organic framework. Thus, an acid aqueous (pH 3) condition was selected for further experiments. The possible reaction in solution during AO7 adsorbed onto MIL-100 (Fe) is shown in Fig. 3 [18,34,35].

3.3. Effect of the dosage of MIL-100 (Fe)

The effect of the dosage of MIL-100 (Fe) was carried out in 10 mL dye solution with the initial concentration at 30 ppm in an acid aqueous condition (pH 3) at 298 K. As shown in Fig. 4 (1), MIL-100 (Fe) could decolor nearly 95% of the 30 mg L^{-1} AO7 aqueous solution within 60 min when the dosage of adsorbent was just reached to 0.8 mg mL^{-1}. The effect of the dosage of MIL-100 (Fe) on the adsorption amount and the decolorization at 4 h is shown in Fig. 4. (2). It can be seen that with the increasing of the dosage of MIL-100 (Fe), the decolorization ratio of AO7 increased obviously, especially when the concentration of MIL-100 (Fe) was below 0.4 mg mL^{-1}, and then it reached an equilibrium value after 0.4 mg mL^{-1}.

It could be attributed to an increase in the adsorbent total surface area, which enlarged the number of adsorption sites available for adsorption. The effect of the dosage of MIL-100 (Fe) on the decolorization of AO7 was similar to our previous report [36]. However, the increase of the dosage of MIL-100 (Fe) was not favorable for the adsorption ability. Dye adsorbed on MIL-100 (Fe) decreased from 109.5 to 32.2 mg g^{-1} at 4 h as the dosage of adsorbent increased from 0.2 to 0.9 mg mL^{-1}. This may be caused by overlapping or aggregation of adsorption sites, resulting in a decrease in the total adsorbent surface area available to dye and an increase in diffusion path length [37]. To be

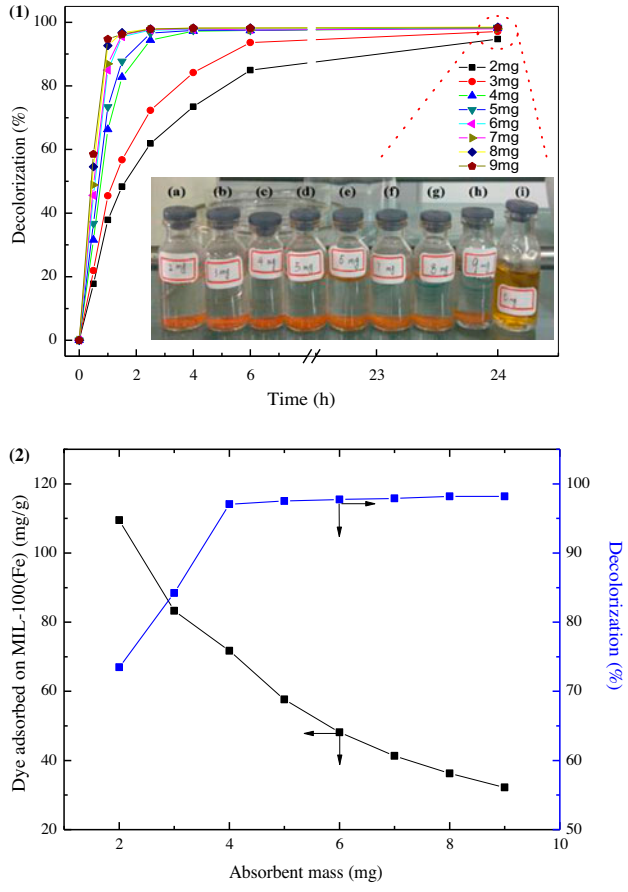

Fig. 4. Effect of the dosage of MIL-100 (Fe) on the decolorization of AO7 at different times: (1) 0–24 h, in which 2 mg (a), 3 mg(b), 4 mg(c), 5 mg(d), 6 mg(e), 7 mg(f), 8 mg(g), 9 mg(h), and 0 mg(i) adsorbent was used; (2) at 4 h.

brief, a relatively high dosage of the adsorbent lead to a high adsorption rate but a low adsorption quantity. In order to make a balance between quick adsorption and high adsorption quantity, the dosage of MIL-100 (Fe) was fixed at 0.4 mg mL^{-1} in the following experiments.

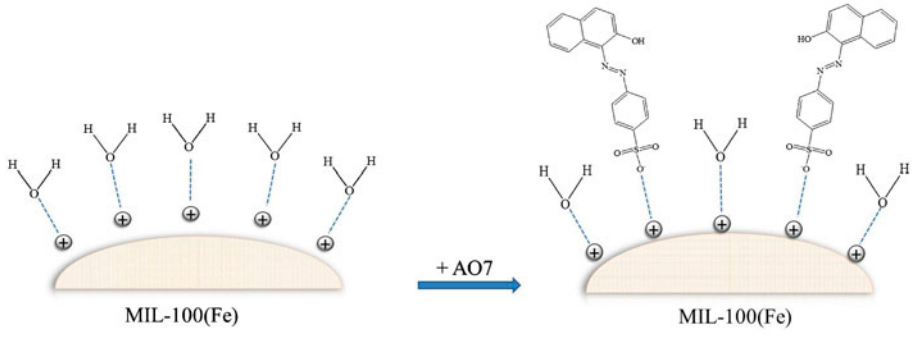

Fig. 3. The possible reaction in solution during AO7 adsorbed onto MIL-100 (Fe).

3.4. Adsorption kinetics

In order to understand the adsorption kinetics, AO7 was adsorbed on MIL-100 (Fe) at various times up to 8 h. To compare the adsorption kinetics precisely, the changes of adsorbed amount with time were treated with the pseudo-second-order kinetic model.

$$\frac{dq_t}{dt} = k_2(q_e - q_t)^2 \tag{2}$$

$$\frac{t}{q_t} = \frac{1}{k_2 q_e^2} + \frac{1}{q_e}t \tag{3}$$

where q_e: amount adsorbed at equilibrium (mg/g), q_t: amount adsorbed at time t (mg/g), and t: adsorption time (h). Therefore, the second-order kinetic constant (k_2) can be calculated by k_2 = slope^2/intercept when the t/q_t was plotted against t.

The adsorption kinetics experiments were conducted at a fixed adsorbent concentration (0.4 mg mL^{-1}) and pH (pH 3) at 298 K at various initial dye concentrations. As shown in Fig. 5(a), the adsorbed amount of AO7 over MIL-100 (Fe) was increased with the increasing of the initial dye concentration. Fig. 5(b) shows the plots of the pseudo-second-order kinetics of the AO7 over MIL-100 (Fe) and the calculated kinetic parameters are shown in Table 1. It can be seen, the correlation coefficients (R^2) were very close to 1 ($R^2 > 0.999$) for every different initial dye concentration, indicating that pseudo-second-order kinetic model was suitable for the adsorption of AO7 over MIL-100 (Fe). The calculated kinetic constants (k_2) decreased at a relatively high dye concentration which was similar to other dyes adsorbed over MOFs. However, the kinetic constant was also higher than other adsorbent.

The adsorption data were also analyzed using the pseudo-first-order kinetic model.

$$\frac{dq_t}{dt} = k_1(q_e - q_t) \tag{4}$$

$$\ln(q_e - q_t) = \ln q_e - k_1 t \tag{5}$$

where q_e: amount adsorbed at equilibrium (mg g^{-1}), q_t: amount adsorbed at time t (mg g^{-1}), t: adsorption time (min). The first-order kinetic constant k_1 can be calculated by k_1 = slope when the ln ($q_e - q_t$) was plotted against t.

But the correlation coefficients (R^2) of the pseudo-first-order kinetic model were far from 1 (shown in Supporting Table S2). So, the pseudo-first-order kinetic model was not suitable to describe the adsorption progress. Briefly, the kinetic constant of the AO7 over MIL-100 (Fe) was not only influenced by the dye concentration but also the adsorbent concentration.

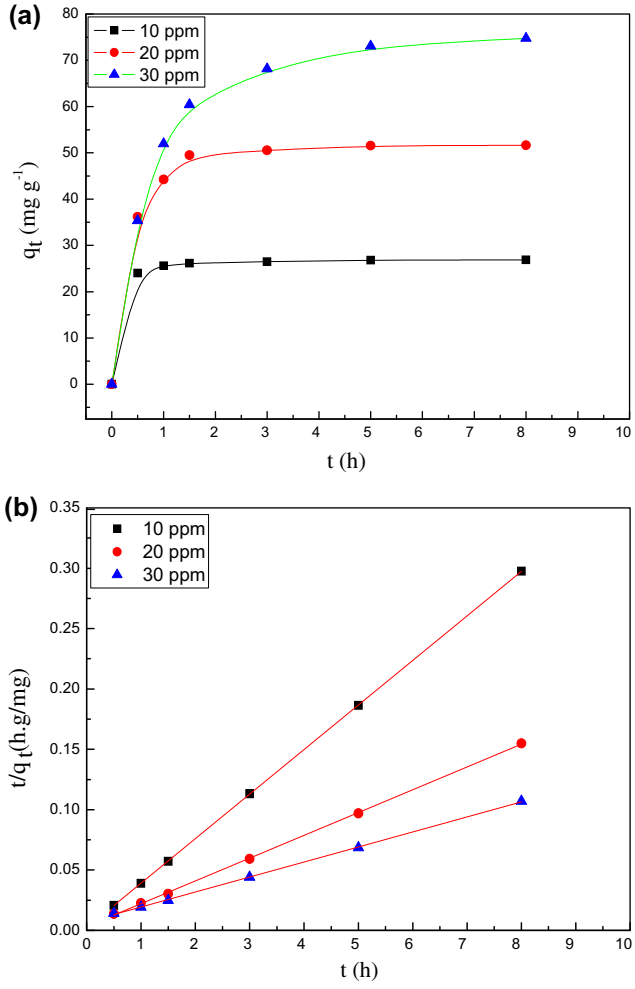

Fig. 5. (a) Effect of contact time and initial AO7 concentration on the adsorption of AO7 over MIL-100 (Fe); (b) Plots of pseudo-second-order kinetics of AO7 adsorption over MIL-100 (Fe).

3.5. Adsorption isotherms

In order to further understand the interactive behavior between adsorbate and adsorbents, the fundamental equilibrium adsorption isotherms were investigated. Adsorption isotherms for AO7 on MIL-100 (Fe) were studied after adsorbing AO7 with different initial dye concentrations (from 50 to 500 ppm) for 72 h at different temperature.

Table 1
Pseudo-second-order kinetics constants of AO7 on MIL-100 (Fe)

Adsorbent	Dye	C_0/(ppm)	Q_e(exp)/(mg g^{-1})	Q_t(cal)/(mg g^{-1})	k_2/(g mg^{-1} h^{-1})	R^2
MIL-100(Fe)	AO7	10	26.89	27.10	0.619	0.9996
		20	51.63	52.97	0.111	0.9994
		30	74.73	80.32	0.0226	0.9995

As shown in Fig. 6, the adsorption quantity increased gradually at relatively low initial dye concentrations and then reached a maximum with the increasing of the dye equilibrium concentrations.

The Langmuir adsorption isotherm model was selected to describe the adsorption isotherm. The equation expressed is:

$$\frac{C_e}{Q_e} = \frac{C_e}{Q_0} + \frac{1}{Q_0 K_L} \tag{6}$$

where Q_e: the equilibrium adsorption capacity of adsorbate (AO7) on the adsorbent (MIL100-(Fe)) (mg g^{-1}), C_e: the equilibrium AO7 concentration in solution (mg L^{-1}), Q_0: Langmuir constant (the maximum adsorption capacity of adsorbent) (mg g^{-1}), and K_L: Langmuir adsorption constant (L mg^{-1} or L mol^{-1}) (related to the free energy of adsorption).

As shown in Fig. 7, a linear plot of (C_e/Q_e) vs. C_e was obtained from Langmuir adsorption isotherm model. Results showed that Langmuir adsorption isotherm model was suitable to describe the adsorption at different temperatures, as the correlation coefficients were all above 0.999 (shown in Table 2). K_L and Q_0 were calculated from the slope and intercept of the different straight lines representing the different temperature, listed in Table 2. The maximum adsorption capacities (Q_0) increased with the rising temperature, indicating the adsorption was an endothermic progress.

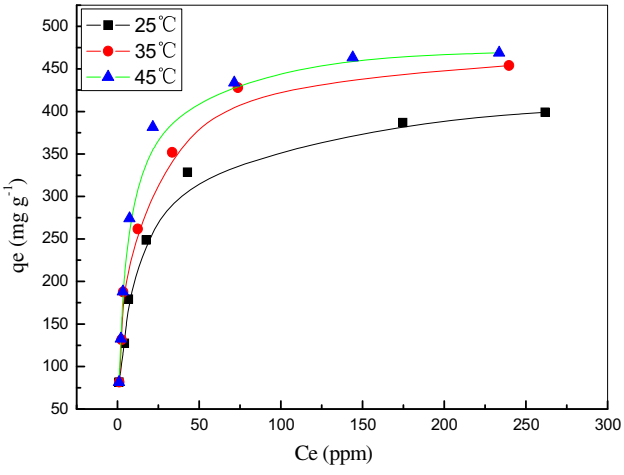

Fig. 6. Adsorption isotherms for MO adsorption over MIL-100 (Fe) at 25, 35, and 45°C.

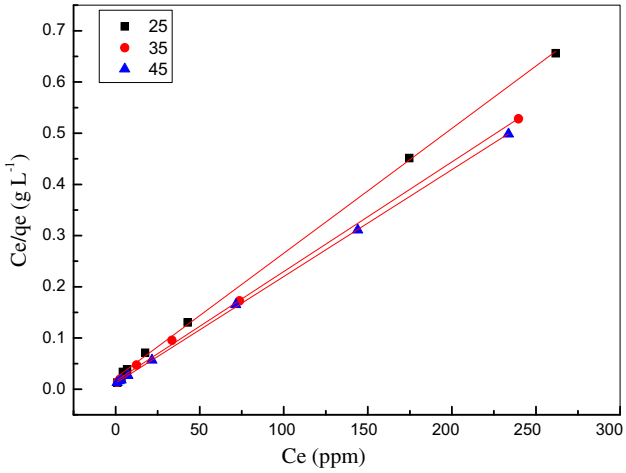

Fig. 7. Langmuir plots of the isotherms.

These results indicated that the adsorption of AO7 onto MIL-100 (Fe) was a typical monomolecular layer adsorption. The comparison of the maximum adsorption abilities of different adsorbents for the removal of AO7 is listed in Supporting Table S3. It can be concluded that, compared to previously used sorbents, MIL-100 (Fe) has comparable adsorption potential for the removal of AO7.

3.6. Adsorption thermodynamics

The adsorption thermodynamics function obtained from the isotherms will further reveal the adsorption mechanism. As shown above, the adsorption isotherms experiments were carried out at 298, 308, and 318 K, respectively. The Langmuir equation was selected to fit the adsorption isotherm. The Gibbs free energy change ΔG^0 can be calculated by the following equation:

Table 2
Parameters of adsorption isotherms for AO7 on the MIL-100 (Fe) at different temperatures

Temprature (℃)	Q_0 (mg g^{-1})	K_L (L mol^{-1})	R^2	ΔG^0 (kJ mol^{-1})	ΔH^0 (kJ mol^{-1})	ΔS^0 (J mol^{-1} K^{-1})
25	409.84	39.23	0.9993	−9.10		
35	467.29	47.84	0.9992	−9.90	1.81	91.17
45	480.77	62.17	0.9998	−10.92		

$$\Delta G^0 = -\mathrm{RT}\ln K_L \quad (\Delta G^0 < 0, \text{spontaneous}) \tag{7}$$

where K_L: the Langmuir adsorption constant (L mol^{-1}).

As shown in Table 2, the calculated K_L was a positive value and increased with the increasing temperature. The negative free energy change (ΔG^0) demonstrated that the adsorption of AO7 on MIL-100 (Fe) was feasible and spontaneous under the adsorption conditions.

$$\text{At the same time, } \Delta G^0 = \Delta H^0 - T\Delta S^0 (\Delta H < 0, \text{exothermic}) \tag{8}$$

So, the enthalpy change ΔH^0 and ΔS^0 can be obtained from the van't Hoff equation:

$$\ln K_L = \frac{\Delta S^0}{R} - \frac{\Delta H^0}{\mathrm{RT}} \tag{9}$$

According to van't Hoff Eq. (9), the van't Hoff plot of ln K_L against 1/T can be made (shown in Fig. 8), then the enthalpy change (ΔH^0) and entropy change (ΔS^0) can be obtained from the (−slope × R) and (intercept × R) of the van't Hoff plot, respectively.

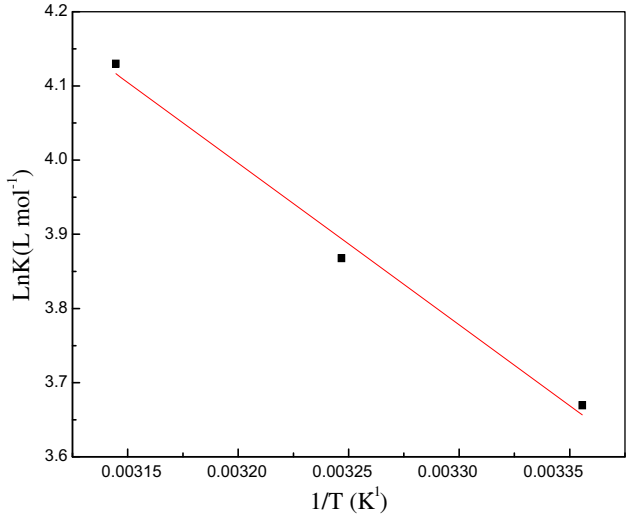

Fig. 8. van't Hoff plots to get the ΔH^0 and ΔS^0 of the AO7 adsorption over the MIL-100 (Fe).

The positive ΔH^0 confirming endothermic adsorption in accord with the increasing adsorption capacity associated with increasing adsorption temperature. The endothermic adsorption may be due to a stronger interaction between pre-adsorbed water and the adsorbent than the interaction between AO7 and the adsorbent. However, further work was necessary to clarify this suggestion. The positive ΔS^0 means the increased randomness with adsorption of AO7 probably because the number of desorbed water molecules was larger than that of the adsorbed AO7 molecules (AO7 was very relatively bulky compared with water; therefore, several water molecules may be desorbed by adsorption of an AO7 molecule). Therefore, the driving force of AO7 adsorption on MIL-100 (Fe) was due to an entropy effect rather than an enthalpy change. The adsorption mechanism may be explained with a simple electrostatic interaction (–SO_3) between AO7 aqueous solution and the adsorbent (as shown in Fig. 3) [34,35]. Once again, the MIL-100 (Fe) shows the potential applications in removing AO7 in the viewpoint of kinetics and adsorption capacity.

4. Conclusion

In this work, MIL-100 (Fe) was synthesized and applied to the removal of organic dyes from the simulated dye wastewater-containing AO7. The results show that the pseudo-second-order kinetic model fits the adsorption progress better compared with the pseudo-first-order kinetic model. Both the adsorbent concentration and the initial dye concentration have an effect on the adsorption kinetics. The change of the Zeta potential and the decolorization ratio of AO7 with a pH value suggested that the key factor of the adsorption might be the charge interactions between dye and adsorbent. The adsorption isotherms at different temperatures obeyed the Langmuir model well. In addition, the calculated thermodynamics parameters suggested that the adsorption of AO7 on MIL-100 (Fe) was a spontaneous and endothermic process, and the driving force of the adsorption was due to an entropy

effect rather than an enthalpy change. From this study, it can be suggested that MOF-type materials can be applied in the adsorptive removal of organic dye in contaminated water.

Supplementary material

The supplementary material for this paper is available online at http://dx.doi.10.1080/19443994.2014.982199.

Acknowledgment

The authors would like to express their appreciation to the National 863 Plans Projects (2012AA06A111), China, and Major Project of Education Department in Hubei Province, China (D20120107) for support of this work.

References

[1] G. Crini, Non-conventional low-cost adsorbents for dye removal: A review, Bioresour. Technol. 97 (2006) 1061–1085.
[2] M. Rafatullah, O. Sulaiman, R. Hashim, A. Ahmad, Adsorption of methylene blue on low-cost adsorbents: A review, J. Hazard. Mater. 177 (2010) 70–80.
[3] V.K. Gupta, Suhas, Application of low-cost adsorbents for dye removal—A review, J. Environ. Manage. 90 (2009) 2313–2342.
[4] S.-A. Ong, L.-N. Ho, Y.-S. Wong, Comparison on biodegradation of anionic dye orange II and cationic dye methylene blue by immobilized microorganisms on spent granular activated carbon, Desalin. Water Treat. (2014) 1–5.
[5] V. Meshko, L. Markovska, M. Mincheva, A.E. Rodrigues, Adsorption of basic dyes on granular acivated carbon and natural zeolite, Water Res. 35 (2001) 3357–3366.
[6] N. Kannan, M.M. Sundaram, Kinetics and mechanism of removal of methylene blue by adsorption on various carbons—A comparative study, Dyes Pigm. 51 (2001) 25–40.
[7] M.S. Lucas, J.A. Peres, Decolorization of the azo dye Reactive Black 5 by Fenton and photo-Fenton oxidation, Dyes Pigm. 71 (2006) 236–244.
[8] A. Zuorro, R. Lavecchia, Evaluation of UV/H_2O_2 advanced oxidation process (AOP) for the degradation of diazo dye Reactive Green 19 in aqueous solution, Desalin. Water Treat. 52 (2014) 1571–1577.
[9] A.A. Adeyemo, I.O. Adeoye, O.S. Bello, Metal organic frameworks as adsorbents for dye adsorption: Overview, prospects and future challenges, Toxicol. Environ. Chem. 94 (2012) 1846–1863.
[10] G. Férey, Hybrid porous solids: Past, present, future, Chem. Soc. Rev. 37 (2008) 191–214.
[11] S. Kitagawa, R. Kitaura, S. Noro, Functional porous coordination polymers, Angew. Chem. Int. Ed. 43 (2004) 2334–2375.
[12] O.M. Yaghi, M. O'Keeffe, N.W. Ockwig, H.K. Chae, M. Eddaoudi, J. Kim, Reticular synthesis and the design of new materials, Nature 423 (2003) 705–714.
[13] H. Furukawa, K.E. Cordova, M. O'Keeffe, O.M. Yaghi, The chemistry and applications of metal-organic frameworks, Science 341 (2013) 1230444-1–1230444-12.
[14] M. Maes, M. Trekels, M. Boulhout, S. Schouteden, F. Vermoortele, L. Alaerts, D. Heurtaux, Y.K. Seo, Y.K. Hwang, J.S. Chang, Selective removal of N-Heterocyclic aromatic contaminants from fuels by lewis acidic metal-organic frameworks, Angew. Chem. 123 (2011) 4296–4300.
[15] N.A. Khan, S.H. Jhung, Remarkable adsorption capacity of $CuCl_2$-loaded porous vanadium benzenedicarboxylate for benzothiophene, Angew. Chem. 124 (2012) 1224–1227.
[16] E. Haque, J.E. Lee, I.T. Jang, Y.K. Hwang, J.S. Chang, J. Jegal, S.H. Jhung, Adsorptive removal of methyl orange from aqueous solution with metal-organic frameworks, porous chromium-benzenedicarboxylates, J. Hazard. Mater. 181 (2010) 535–542.
[17] L. Li, J.C. Li, Z. Rao, G.W. Song, B. Hu, Metal organic framework $[Cu_3(BTC)_2(H_2O)_3]$ for the adsorption of methylene blue from aqueous solution, Desalin. Water Treat. (2013) 1–7.
[18] B.K. Jung, Z. Hasan, S.H. Jhung, Adsorptive removal of 2,4-dichlorophenoxyacetic acid (2,4-D) from water with a metal-organic framework, Chem. Eng. J. 234 (2013) 99–105.
[19] C.Y. Huang, M. Song, Z.Y. Gu, H.F. Wang, X.P. Yan, Probing the adsorption characteristic of metal-organic framework MIL-101 for volatile organic compounds by quartz crystal microbalance, Environ. Sci. Technol. 45 (2011) 4490–4496.
[20] H. Sato, W. Kosaka, R. Matsuda, A. Hori, Y. Hijikata, R.V. Belosludov, S. Sakaki, M. Takata, S. Kitagawa, Self-accelerating CO sorption in a soft nanoporous crystal, Science 343 (2014) 167–170.
[21] F. Ke, L.G. Qiu, Y.P. Yuan, F.M. Peng, X. Jiang, A.J. Xie, Y.H. Shen, J.F. Zhu, Thiol-functionalization of metal-organic framework by a facile coordination-based postsynthetic strategy and enhanced removal of Hg^{2+} from water, J. Hazard. Mater. 196 (2011) 36–43.
[22] H.K. Chae, D.Y. Siberio-Pérez, J. Kim, Y. Go, M. Eddaoudi, A.J. Matzger, M. O'Keeffe, O.M. Yaghi, A route to high surface area, porosity and inclusion of large molecules in crystals, Nature 427 (2004) 523–527.
[23] F. Leng, W. Wang, X.J. Zhao, X.L. Hu, Y.F. Li, Adsorption interaction between a metal–organic framework of chromium–benzenedicarboxylates and uranine in aqueous solution, Colloids Surf. A 441 (2014) 164–169.
[24] C. Chen, M. Zhang, Q. Guan, W. Li, Kinetic and thermodynamic studies on the adsorption of xylenol orange onto MIL-101(Cr), Chem. Eng. J. 183 (2012) 60–67.
[25] S.-H. Huo, X.-P. Yan, Metal-organic framework MIL-100(Fe) for the adsorption of malachite green from aqueous solution, J. Mater. Chem. 22 (2012) 7449–7455.
[26] E. Haque, J.W. Jun, S.H. Jhung, Adsorptive removal of methyl orange and methylene blue from aqueous solution with a metal-organic framework material, iron terephthalate (MOF-235), J. Hazard. Mater. 185 (2011) 507–511.

[27] N.A. Khan, Z. Hasan, S.H. Jhung, Adsorptive removal of hazardous materials using metal-organic frameworks (MOFs): A review, J. Hazard. Mater. 244–245 (2013) 444–456.
[28] C.K. Lim, H.H. Bay, C.H. Neoh, A. Aris, Z.A. Abdul Majid, Z. Ibrahim, Application of zeolite-activated carbon macrocomposite for the adsorption of Acid Orange 7: Isotherm, kinetic and thermodynamic studies, Environ. Sci. Pollut. Res. 20 (2013) 7243–7255.
[29] A. Ashori, Y. Hamzeh, A. Ziapour, Application of soybean stalk for the removal of hazardous dyes from aqueous solutions, Polym. Eng. Sci. 54 (2014) 239–245.
[30] V. Gupta, A. Mittal, V. Gajbe, J. Mittal, Removal and recovery of the hazardous azo dye acid orange 7 through adsorption over waste materials: Bottom ash and de-oiled soya, Ind. Eng. Chem. Res. 45 (2006) 1446–1453.
[31] M. Kousha, E. Daneshvar, M.S. Sohrabi, M. Jokar, A. Bhatnagar, Adsorption of acid orange II dye by raw and chemically modified brown macroalgae *Stoechospermum marginatum*, Chem. Eng. J. 192 (2012) 67–76.
[32] J.W. Yoon, Y.K. Seo, Y.K. Hwang, J.S. Chang, H. Leclerc, S. Wuttke, P. Bazin, A. Vimont, M. Daturi, E. Bloch, P.L. Llewellyn, C. Serre, P. Horcajada, J.M. Grenèche, A.E. Rodrigues, G. Férey, Controlled reducibility of a metal-organic framework with coordinatively unsaturated sites for preferential gas sorption, Angew. Chem. Int. Ed. 49 (2010) 5949–5952.
[33] M. Tong, D. Liu, Q. Yang, S. Devautour-Vinot, G. Maurin, C. Zhong, Influence of framework metal ions on the dye capture behavior of MIL-100 (Fe, Cr) MOF type solids, J. Mater. Chem. A 1 (2013) 8534–8537.
[34] M. Arshadi, F. Salimi Vahid, J.W.L. Salvacion, M. Soleymanzadeh, Adsorption studies of methyl orange on an immobilized Mn-nanoparticle: Kinetic and thermodynamic, RSC Adv. 4 (2014) 16005–16017.
[35] M. Arshadi, F. Salimi Vahid, J.W.L. Salvacion, M. Soleymanzadeh, A practical organometallic decorated nano-size SiO_2-Al_2O_3 mixed-oxides for methyl orange removal from aqueous solution, Appl. Surf. Sci. 280 (2013) 726–736.
[36] F.-C. Tsai, N. Ma, T.-C. Chiang, L.-C. Tsai, J.-J. Shi, Y. Xia, T. Jiang, S.-K. Su, F.-S. Chuang, Adsorptive removal of methyl orange from aqueous solution with crosslinking chitosan microspheres, J. Water Process. Eng. 1 (2014) 2–7.
[37] X.J. Li, L.Y. Zheng, L.Z. Huang, O. Zheng, Z.Y. Lin, L.H. Guo, B. Qiu, G.N. Chen, Adsorption removal of crystal violet from aqueous solution using a metal-organic frameworks material, copper coordination polymer with dithiooxamide, J. Appl. Polym. Sci. 129 (2013) 2857–2864.